GULF STATES UTILITIES COMPANY
POST OFFICE BOX 2951 • BEAUMONT, TEXAS 77704
AREA CODE 713 838-6631

March 1, 1985
RBG- 20,270
File No. G9.5, G9.8.6.2

Mr. Harold R. Denton, Director
Office of Nuclear Reactor Regulation
U.S. Nuclear Regulatory Commission
Washington, D.C. 20555

Dear Mr. Denton:

River Bend Station - Unit 1
Docket No. 50-458

Enclosed is the Gulf States Utilities Company (GSU) response to the letter from Mr. A. Schwencer (NRC) to Mr. W. J. Cahill (GSU) dated January 25, 1985. Attachment 1 provides a summary of each response to your questions and comments on pool dynamic loads for River Bend Station (RBS). Enclosure 1 provides revised pages, tables and figures from the Final Safety Analysis Report (FSAR) which supports the responses in Attachment 1. These revisions to the FSAR will be included in a future amendment and supply the requested information necessary to close-out Safety Evaluation Report (SER) Outstanding Issue No. 7.

Sincerely,

J. E. Booker

J. E. Booker
Manager-Engineering
Nuclear Fuels & Licensing
River Bend Nuclear Group

JEB/WJR/JWL/je

Attachment (1)

Enclosure (1)

A001
1/40

ATTACHMENT 1

1. Section 6A.8: Loads on Structures in the Suppression Pool

Except for the vent clearing jet load (Section 6A8.1.1), the applicant indicates that the GESSAR II methodology was employed to develop all design loads. However, it is not stated explicitly that the limitations and/or modification to these methods as required by the staff's acceptance criteria (Section 2.0 of Appencix C of NUREG-0978) have been incorporated. Have these modifications been incorporated? If they have not, what is the justification for their neglect?

Response:

The RBS submerged structure load calculation procedure is based on the method developed in GESSAR but modified in accordance with the NUREG-0978 acceptance criteria (Appendix C, Section 2.0). In particular, circumscribed cylinders were used for non-cylindrical structures, and standard drag was calculated and combined with the acceleration drag for LOCA bubble and condensation oscillation loads. In accordance with the Mark I and Mark II acceptance criteria, structures were divided into small segments to obtain more precise flow field values. The velocity and acceleration at the geometrical center of each of the structure elements were used to calculate the standard and acceleration drag. The standard drag was determined from Morrison's equation with a standard drag coefficient not less than 1.2. The standard drag coefficient of 1.2 was used for stand-alone structures. If structures were found in the vicinity of each other, interference effects were evaluated in accordance with Mark II procedures. Corresponding revisions to Attachment L, Sections L.6A.2.3 and L.6A.2.6, are contained in Enclosure 1.

2. Section 6A.10.1: Impact Loads

The pressure amplitude for short ($x < 4$ ft) circumferential structures is not determined correctly. The method outlined can lead to an incorrect impulse of impact. Please refer to "Suggested Acceptance Criteria for Impact Loads on Short Mark III Structures Close to the Pool" by G. Maise, February 15, 1984.

Response:

For radial and circumferential strcutures within 6 feet of the pool surface, the pressure amplitudes are first adjusted based on Equation 3-7 of NUREG-0978. The pulse durations are reduced based on procedures described in G. Maise's "Suggested Acceptance Criteria for Impact Loads on Short Mark III Structures Close to the Pool", February 15, 1984. The final impact pressure is then found by equating the impulse for the 0.007 second duration with that for the reduced pulse duration:

$$p' = \frac{Pmax\ H^2}{100} \left(2.6 - 1.6\sqrt{\frac{H}{10}}\right)^2$$

$$p\tau = p' \ (0.007)$$

Where τ is the pulse duration found by the method of G. Maise.

See revised Section 6A.10.1 contained in Enclosure 1.

3. Section 6A.10.1: Drag Loads

The abcissa of Figure 6A.10-5 must start at 1.0 and not at 0 as drawn. Note that the lowest pressure drag is observed on a square plate, a/b = 1.0 and it increases as this ratio becomes either larger or smaller than 1. Thus, in the limit of a/b = 0, one has an infinite strip with a drag coefficient of 2.0 and a pressure differential of 21.6 psi (for V = 40 ft/sec). The figure does not show this.

Response:

See revised Figure 6A.10-5 contained in Enclosure 1. The zero (0) is changed to one (1).

4. Section 6A.12: Loads on Structures at and Above the HCU Floor Elevation

The note on Figure 6A.11-1 indicating that the pulse duration for impact cannot be less than 50 msec, is misleading. This applies only to radial structures that span the entire pool annulus. The statement in the text on page 6A.12-1 is correct, however, the use of Figure 6A.11-1, by itself, can lead to errors.

Response:

See revised Figure 6A.11-1 contained in Enclosure 1. The note has been clarified.

5. Section L.6A.2.3: LOCA Bubble Loads

(i) On page L.6A-7 there appears a factor K whose value is not specified. GSU should provide a description of how this parameter is to be evaluated.

(ii) Also on page L.6A-7, unlike the GESSAR II load specification (Section 3B6.2.3), the RBS FSAR does not account explicitly for the effects of multiple bubbles. This would appear to be a nonconservatism for which justification should be provided.

Response:

(i) The K factor used in the LOCA bubble submerged structure load calculation is based on Attachment L Reference 3, which is the same as that used in GESSAR (see GESSAR Reference 24).

RBS-specific values of K as a function of time are provided in Table L.6A-1. See revised Attachment L, Section L.6A.2.3, Item 9 contained in Enclosure 1.

(ii) To account for the effects of multiple bubbles, an extra summation is placed in front of Equation L.6A-5. RBS has used the whole suppression pool in calculating loads on submerged structures and has included the effects of multiple bubbles in the formulation.

6. Table 6A.1-1

(i) The froth impingement load for expansive structures is given as 15 psi for 100 msec. This should be corrected.

(ii) The load specifications for submerged structure drag and fall back loads are not included in this table. Please explain.

Response:

(i) See revised Table 6A.1-1, Sheet 10 of 11 contained in Enclosure 1. The entry for froth impingement load for expansive structures has been corrected.

(ii) See revised Table 6A.1-1, Sheet 7 of 11 contained in Enclosure 1. Entries for submerged structure drag load velocities have been added.

7. Miscellaneous

(i) Figure 6A.5-1 (corresponding to GESSAR Figure 42) does not contain the Figure 42 comment regarding the SRV & drywell air carryover load combination. Please explain.

(ii) Same question for Figure 6A.6-1 (corresponding to GESSAR Figure 48).

Response:

(i) Figure 6A.5-1 has been revised to add the asterisked note (*) that appears on the corresponding GESSAR Figure 3B-42.

(ii) This question was withdrawn by the NRC (Mel Fields) in a telephone conference Monday, January 28, 1985.

Other miscellaneous corrections and revisions to Appendix 6A are also contained in Enclosure 1.

TABLE 6A.1-1 (Cont)

Load	Specified for Design	Engr'g Estimate	Design Basis: Analysis	Design Basis: GE PSTF Test	Section	Comments	
Chugging				5707	6A.4.1.9.2	See GESSAR Table 3B-4 for duration and frequency	15
1. Pre-chug under-pressure	-1.8 psid (peak) -1.34 psid (mean)	-1.5 psid (peak -0.7 psid (mean)				See GESSAR Fig. 3B-28 through 3B-31 for basemat attenuation	15
2. Pulse (spike)	10 psid (peak) 2.4 psid (mean)	7.5 psid (peak) 2 psid (mean)					
3. Post-chug oscillation	±2.1 psid (peak) ±1.3 psid (mean)	±2.0 psid (peak) ±1.0 psid (mean)					
Structure: Basemat							
Break size: Intermediate							
ADS					6A.7.0	See Attachment A	15
Chugging					6A.4.1.9	Same as large break specification	15
Structure: Basemat							
Break size: Small							
Chugging					6A.4.1.9	Same as large break specification	15
Structure: Submerged structures							
Break size: Large (3)							
LOCA water jet loads					Attachment L		15
LOCA air bubble load		8.2 psid	Attachment L		Attachment L		15

INSERT

ENCLOSURE 1

TABLE 6A.1-1 (Cont)

Load	Specified for Design	Engr'g Estimate	Design Basis: Analysis	Design Basis: GE PSTF Test	Section	Comments
Velocity for computing drag loads	50 ft/sec (maximum)	30 ft/sec	Bounding calculation			See Attachment M
Fall back velocity for drag loads	35 ft/sec	20 ft/sec	Bounding calculation		L.6A.2.4	

INSERT for Table 6A.1-1 Sheet 7 of 11

TABLE 6A.1-1 (Cont)

Load	Specified for Design	Engr'g Estimate	Design Basis: Analysis	Design Basis: GE PSTF Test	Section	Comments	
LOCA condensation oscillation loads		0.7 psid	Attachment L		Attachment L		15
LOCA chugging loads		1.9 psid	Attachment L		Attachment L		15
X-Quencher water jet load		Negligible	Attachment L		Attachment L	Load is negligible outside a sphere circumscribed by the quencher arms	15
X-Quencher air bubble load		0.5 psid	Attachment L		Attachment L		15
Structure: Submerged Structures							
Break size: Intermediate (3)							
ADS						See Attachment L	15
Structure: Submerged Structures							
Break size: Small (3)							
No additional loads generated							
Structure: Structures at pool surface							
Break size: Large							
Bubble formation							
Drywell	21.8 psid	18 psi	Equal to D.W. pressure		6A.9.0	Large structures only	15
Containment	10.0 psid		Attentuated D.W. pressure				
Velocity for computing drag loads	~~50 (max)~~ 40 ft/sec	30 ft/sec	Bounding calculation		6A.9.0		15

TABLE 6A.1-1 (Cont)

Load	Specified for Design	Engr'g Estimate	Design Basis: Analysis	Design Basis: GE PSTF Test	Section	Comments	
Structure: Structures between pool surface and HCU floor							
Break size: Small							
No additional loads generated						(See large break tabulation)	
Structure: Expansive Structures at HCU floor elevation							
Break size: Large							
Wetwell pressurization	11 psig (3-4 sec)	3-5 psig (1-2 sec)	LOCTVS	5801, 5802 5803, 5804	6A.11.0		15
Froth impingement	~~Varies~~ ~~15 psig~~ ~~(100 ms)~~	10 psig ~~(100 ms)~~		5801, 5802 5805, 5706	6A.11.0		15
Flow pressure differential	11 psig	3-5 psig	LOCTVS	5801, 5802 5803, 5804	6A.12.0	Test shows pressure differential of 3 to 5 psi	15
Fallback and water accumulation	1 psi	0.5 psi	Bounding calculation		6A.12.0	Based on water flow through HCU floor	15
Structure: Expansive Structures at HCU floor elevation							
Break size: Intermediate							
No additional loads generated						See large break tabulation	
Structure: Expansive Structures at HCU Floor elevation							
Break size: Small							
No additional loads generated						See large break tabulation	
Structure: Small Structures at HCU elevation							
Froth impingement	Varies	10 psid		5801, 5802 5805, 5706	6A.12.0	See Fig. 6A.12-1	15

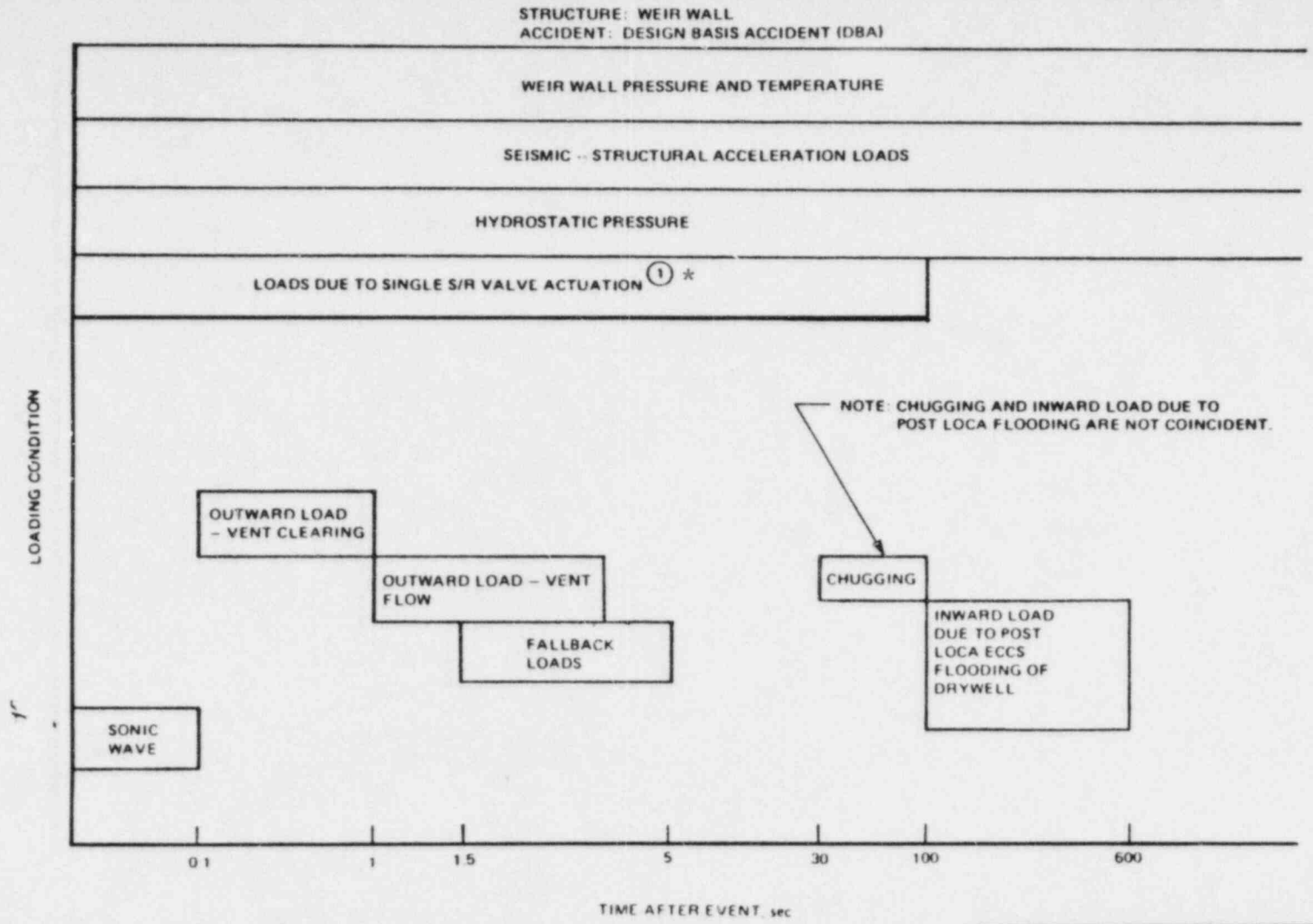

(1) APPLIES TO BOTTOM 2 VENTS ONLY

* Add S/R dynamic load to static load due to drywell air purged to containment

REF.: GESSAR FIG. 3B-42

FIGURE 6A.5-1

WEIR WALL-LOADING CHART FOR DBA

RIVER BEND STATION
FINAL SAFETY ANALYSIS REPORT

6A.6.1.5 Local Containment Loads Resulting from Structures at or Near the Pool Surface

Any structures in the containment annulus that are at or near the suppression pool surface experience upward loads during pool swell. If these structures are attached to the containment wall, then the upward loads are transmitted into the containment wall. Sections 6A.9 and 6A.10 discuss the types of loads that will be transmitted.

Localized loads on the containment wall resulting from the pressure losses associated with water flowing past a body are depicted on Fig. 6A.6-6. Data presented in this figure are based on drag-type calculations and must be multiplied by $(V/40)^2$ if the pool swell velocity is greater than 40 ft/sec as calculated in Section ~~6A.10.2~~ 6A.10.1.

In addition, there will be impact forces on these attached structures unless the lower surface is immersed in the pool before pool swell. The half-wedge protrusion has an applied impact load time history as shown on Fig. 6A.6-7. The velocity of impact (V) (from Section 6A.10.1) is taken to the height where the wedge is first fully submerged, i.e., upper surface. If the lower surface is initially submerged, the abscissa of Fig. 6A.6-7 is replaced by (Vt/h), where h is the unsubmerged height of the wedge. If the wedge angle is not 45 deg, the following ratios are used when applying Fig. 6A.6-7: 15

$$\frac{F_\beta}{F_{45}} = \left[\frac{(\beta)}{(90 - \beta)}\right]^2 \cot \beta$$

$$\frac{t_\beta}{t_{45}} = \cot \beta$$

For horizontal ledges, the impact forces are calculated in the following manner:

1. The force will have a triangular shape as shown in Fig. 6A.6-8.

2. The hydrodynamic mass ~~is~~ of impact (per unit area) for flat targets from Fig. 6-8 of Reference 4 using b (not b/2) for target width.

3. Calculate the impulse using the following equation:

$$I_P = \frac{M_H}{A} V * \frac{1}{(32.2)\ (144)}$$

Where:

I_P = Impulse per unit area, psi-sec

$\frac{M_H}{A}$ = Hydrodynamic mass per unit area, lbm/ft, from (2) above

V = Impact velocity, ft/sec, determined according to Section ~~6A.10.2~~ 6A.10.1

4. Calculate the pulse duration from the equation:

$$\tau = 0.02\ H/V\ (b/2)$$

Where:

τ = Pulse duration, sec

H = Height above pool, ft

b/2 = Width of ledge, ft

V = Impact velocity, ft/sec, determined according to Section ~~6A.10.2~~ 6A.10.1

5. The value of P_{max} will be obtained using the following equation:

$$P_{max} = 2\ I_P / \tau$$

Where:

P_{max} = Peak pressure, psi

6A.6.1.6 Containment Load Due to Pool Swell at the HCU Floor

This structure is approximately 22 ft above the pool surface and is 10 ft above the point where breakthrough occurs. Froth reaches the HCU floor approximately 1/2 sec after top vent clearing and generates both impingement loads on the structures and a flow pressure differential as it passes through the restricted annulus area at this elevation.

The impingement results in vertical loads on the containment wall from any structures attached to it, and the flow pressure differential results in an outward pressure loading on the containment wall at this location. For design, impingement loads as described in Sections 6A.11 and 6A.12

6A.9 LOADS ON STRUCTURES AT THE POOL SURFACE

As described in Reference 1 (Section 3B.9), with the following exception:

For pool swell drag loads produced by water flowing vertically past the structures, a pool swell velocity of 50 ft/sec is used. 15

6A.10 LOADS ON STRUCTURES BETWEEN THE POOL SURFACE AND THE HCU FLOORS

As described in Reference 1 (Section 3B.10).

6A.10.1 Impact Loads

All structures (e.g., beams and pipes) in the annulus above the suppression pool within 18 ft above the pool have widths less than 20 in. Impact loads due to bulk pool swell on these structures are as shown in Fig. 6A.10-2. All beams and pipes experiencing these impact loads fall within the conservative range as defined in GESSAR Fig. 3B.33-1 through Fig. 3B.33-4, with the pulse duration τ and pressure amplitude adjusted as follows:

Insert 1

1. Radial-oriented structures

Delete and replace with Insert 2

$\tau = 7\ (x/4)$ millisec for $x < 4$ ft and $y \geq 6$ ft

$\tau = 7$ millisec for $x \geq 4$ ft and $y \geq 6$ ft

Where x = the length of the structure (ft)

y = elevation above the pool surface (ft)

If the structure is less than 6 ft above the pool surface, τ is reduced by $y/6$.

The pressure amplitude is increased by a factor of $7/\tau$.

15

2. Circumferential-oriented structures

Delete and replace with Insert 3

$\tau = 2\ (x/4)$ millisec

The pressure amplitude is increased by a factor of $2/\tau$.

There are no impact loads on gratings. The width of the grating surfaces does not sustain an impact load.

For structures between 18 and 19 ft above the pool surface, the impact load is interpolated between the values described above and the froth impact loading described in Section 6A.12. The duration is also interpolated from 0.007 sec at 18 ft to 0.100 sec at 19 ft. Fig. 6A.10-3 demonstrates this transition.

Insert 1 for page 6A.10-1

For structures less than 10 feet above the pool surface, the impact pressure can be reduced by:

$$\frac{p'}{Pmax} = \frac{H^2}{100} \left(2.6 - 1.6 \sqrt{\frac{H}{10}}\right)^2$$

where H is the distance above the pool surface.

Insert 2 for page 6A.10-1

a. For structures within 6 feet of the pool surface, the pulse duration τ_1 is given in Figure 6A.10-7.

b. For structures less than 4 feet in length, the pulse duration τ_2 is given in Figure 6A.10-8.

c. For structures both less than 4 feet in length and within 6 feet of the pool surface, the pulse duration is given by:

$$\tau = (\tau_1 \times \tau_2)/0.007$$

d. The value of τ need not be less than that calculated by:

Cylindrical targets

$$\tau = 0.0463\ D/V$$

Flat targets

$$\tau = 0.011\ W/V \text{ for } V \geq 7 \text{ ft/sec}$$
$$\tau = 0.0016\ W \text{ for } V < 7 \text{ ft/sec}$$

where: τ = pulse duration
D = diameter of target (ft)
W = width of flat structure (ft)
V = impact velocity (ft/sec)

e. The pressure load is increased if the duration τ is less than 0.007 seconds. This increase is given by:

$$p = p' (0.007/\tau)$$

where:

p' = the peak pressure shown in Figure 6A.10-2, adjusted as noted above for structures within 10 feet of the pool surface.

Insert 3 for page 6A.10-1

a. For structures within 6 feet of the pool surface, the pulse duration τ is given in Figure 6A.10-9.

b. For structures greater than 6 feet above the pool surface, the pulse duration of Figure 6A.10-2 is used as long as the criteria of GESSAR Figures 3B.33-3 and 3B.33-4 are met.

c. The value of τ need not be less than that calculated by:

Cylindrical targets

$\tau = 0.0463\ D/V$

Flat targets

$\tau = 0.011\ W/V$ for $V \geq 7$ ft/sec
$\tau = 0.0016\ W$ for $V < 7$ ft/sec

where τ, D, W and V are defined as above.

d. If τ is less than 0.007 seconds, the pressure amplitude is increased by:

$p = p' (0.007/\tau)$

where p' is defined as above.

NOTES:
DYNAMIC LOAD OF 0.5 SEC DURATION
APPLIES TO FLAT PLATES
FOR OTHER SHAPES SEE FIGURE 6A.10-6

SOURCE:
MARKS MECHANICAL ENGINEERS HANDBOOK,
SIXTH EDITION, PAGES 11-82

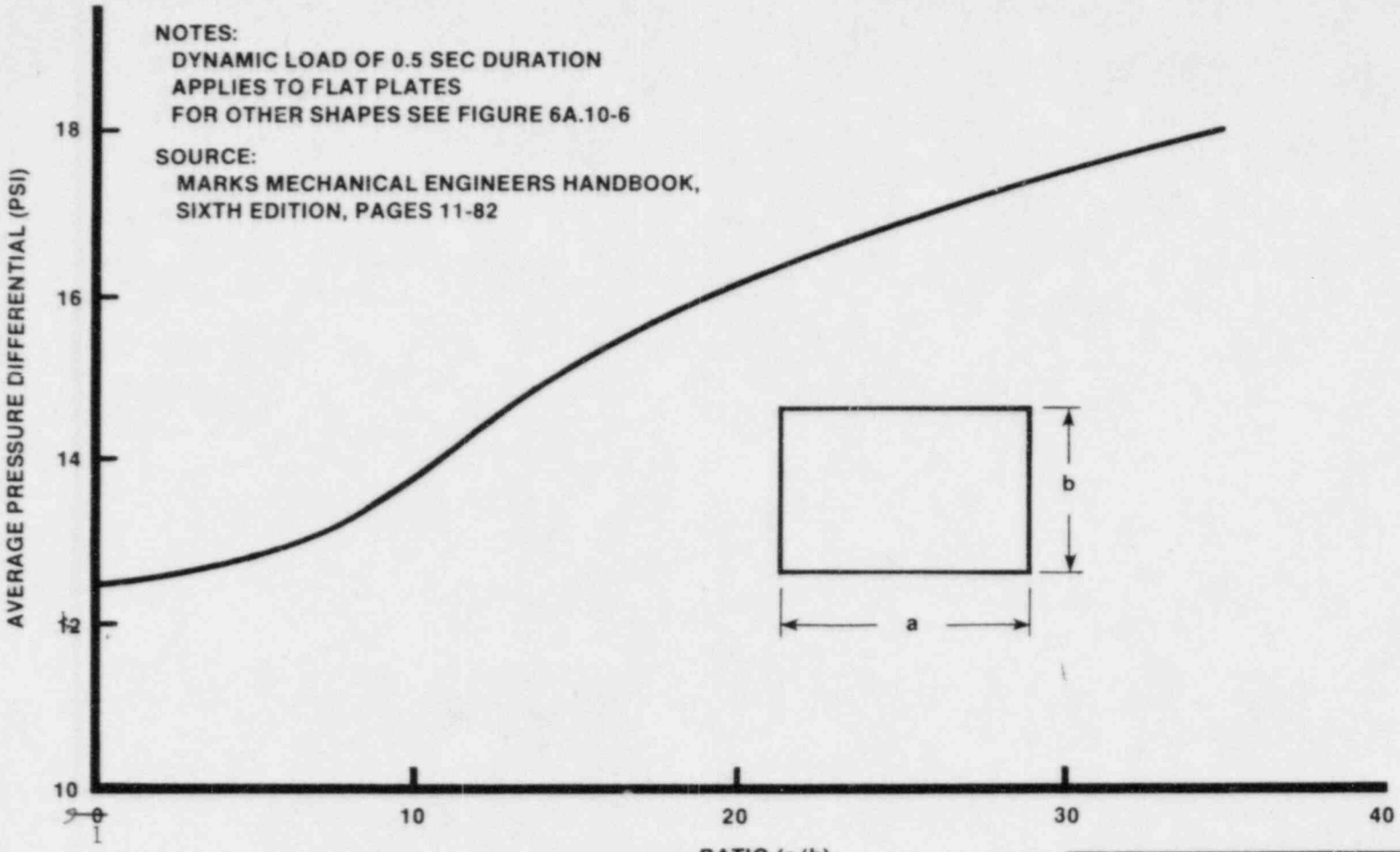

REF.: GESSAR FIG. 3B-76

FIGURE 6A.10-5

DRAG LOAD
ON SOLID STRUCTURES WITHIN
18 FEET OF THE POOL SURFACE

RIVER BEND STATION
FINAL SAFETY ANALYSIS REPORT

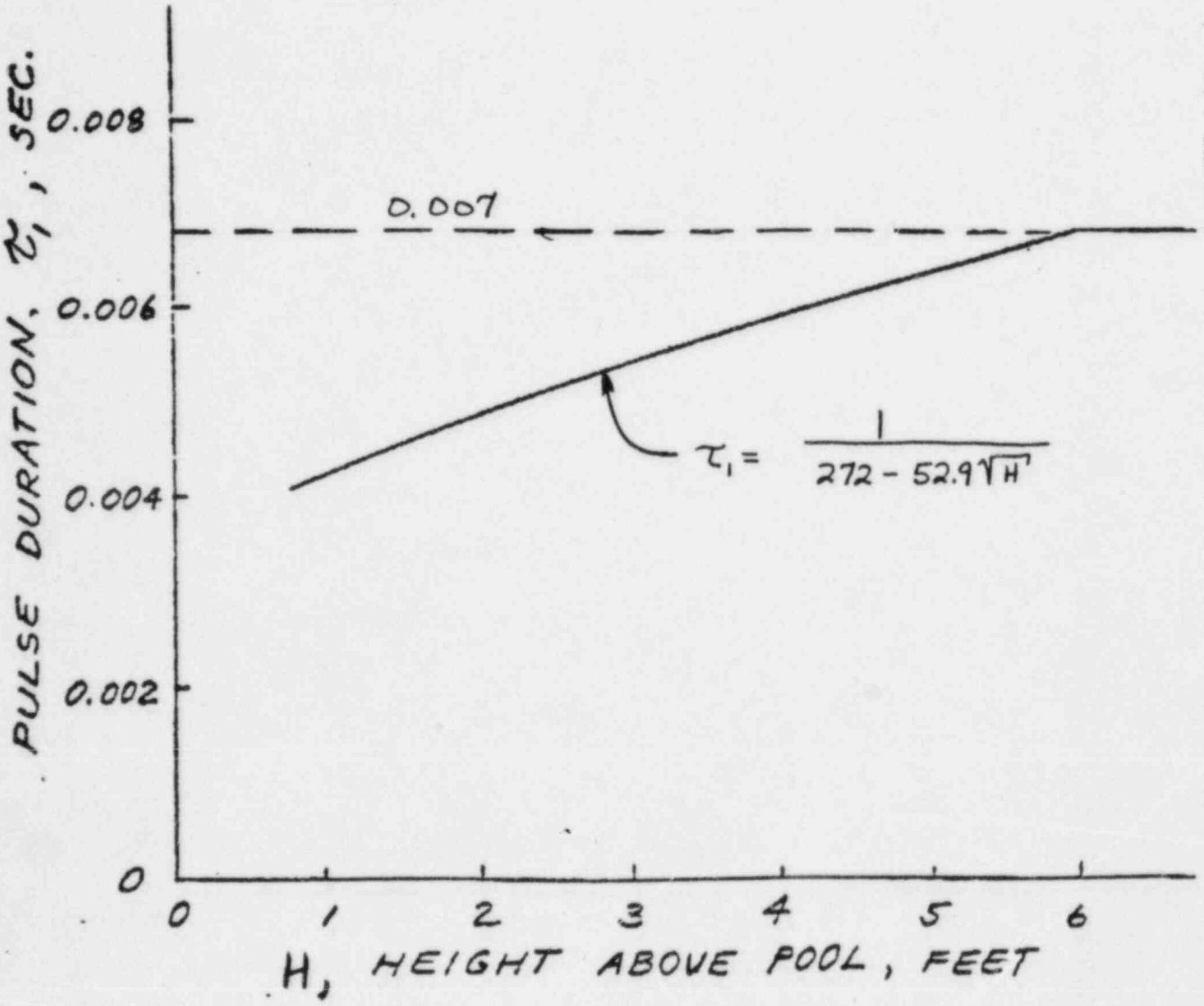

Fig. 6A.10-7

Reduction in pulse duration for radial structures closer than 6 feet to the pool surface.

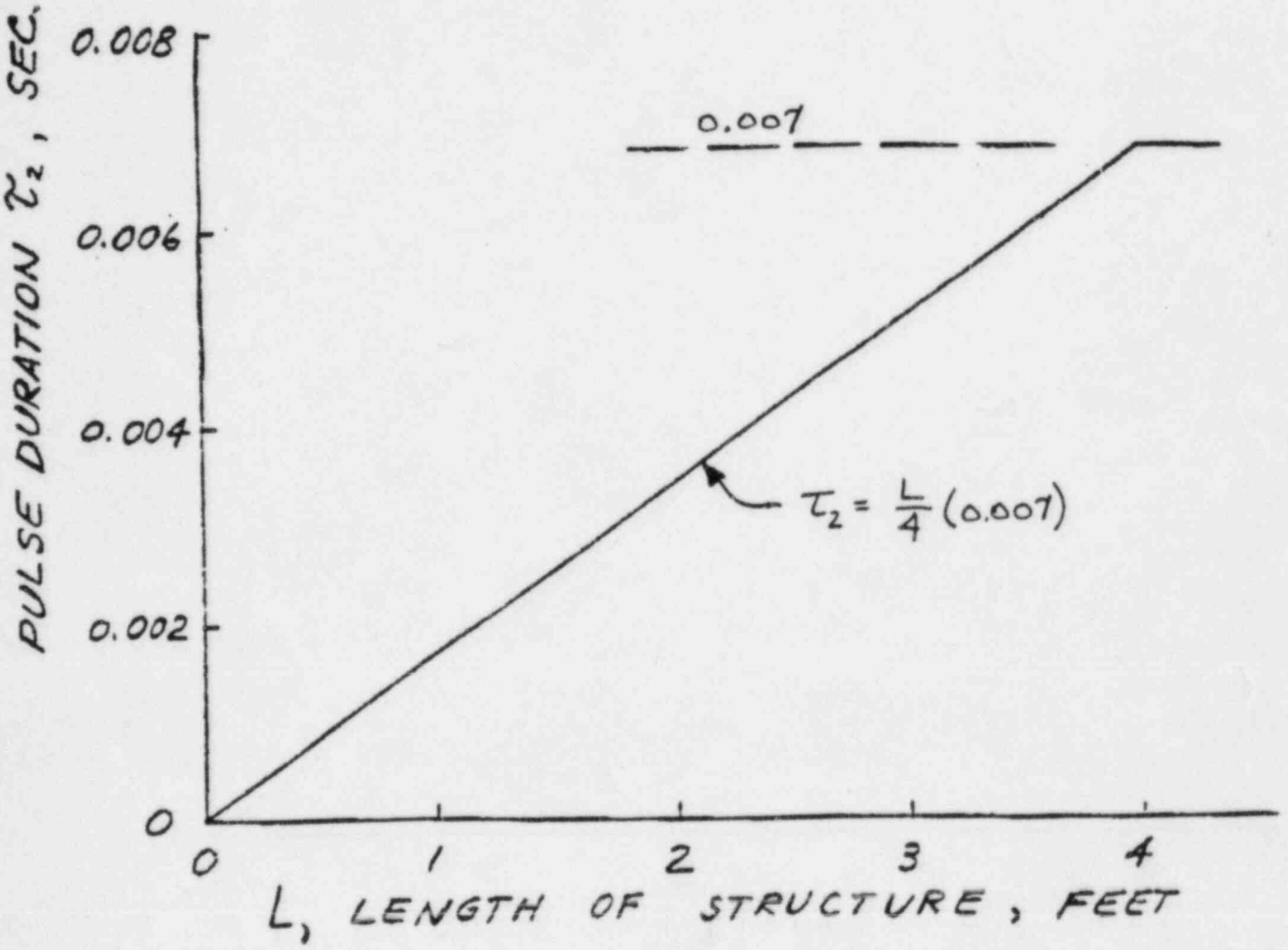

Fig. 6A.10-8

Reduction in pulse duration for radial structures shorter than 4 feet.

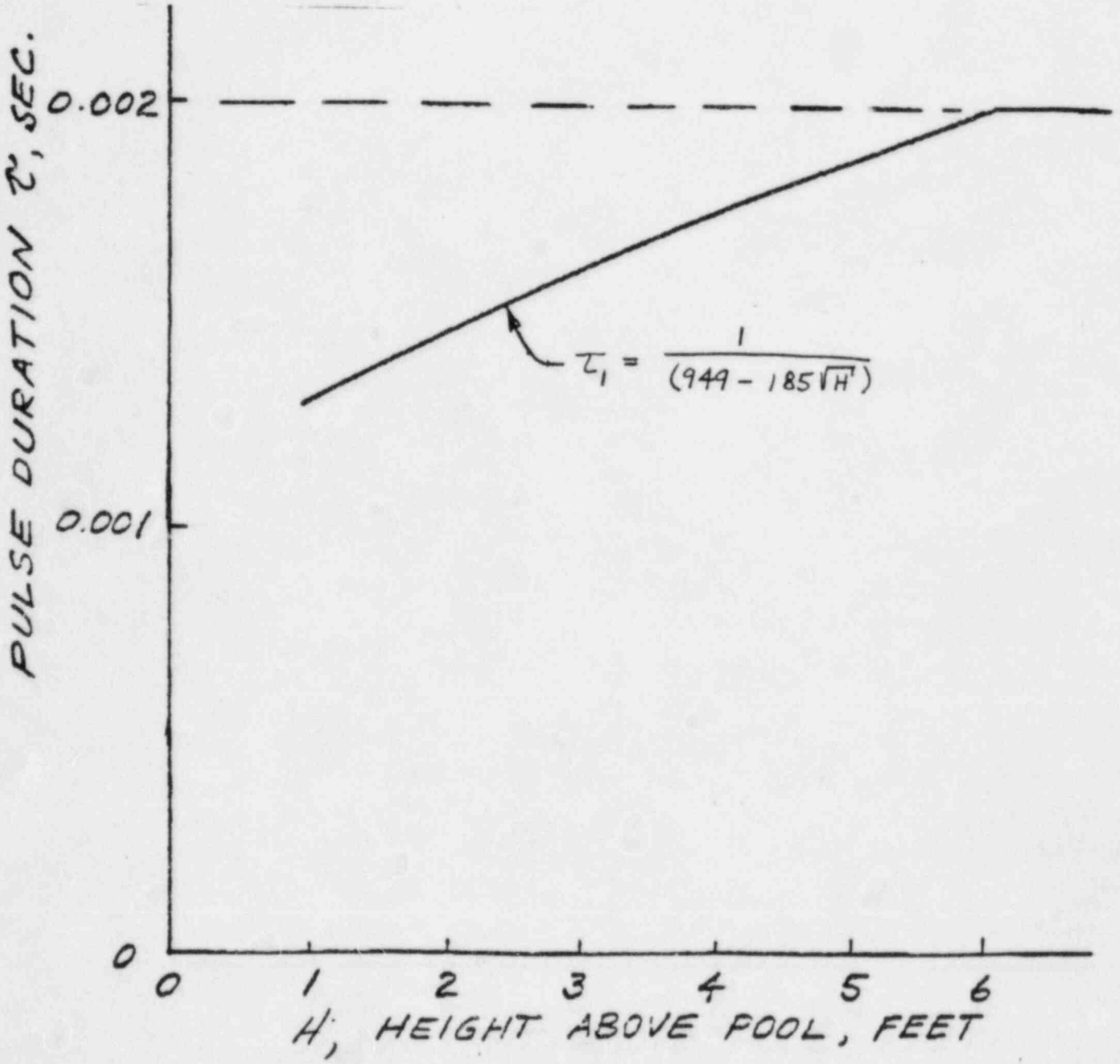

Fig. 6A.10-9

Reduction in pulse duration for circumferential targets closer than 6 feet to the pool surface.

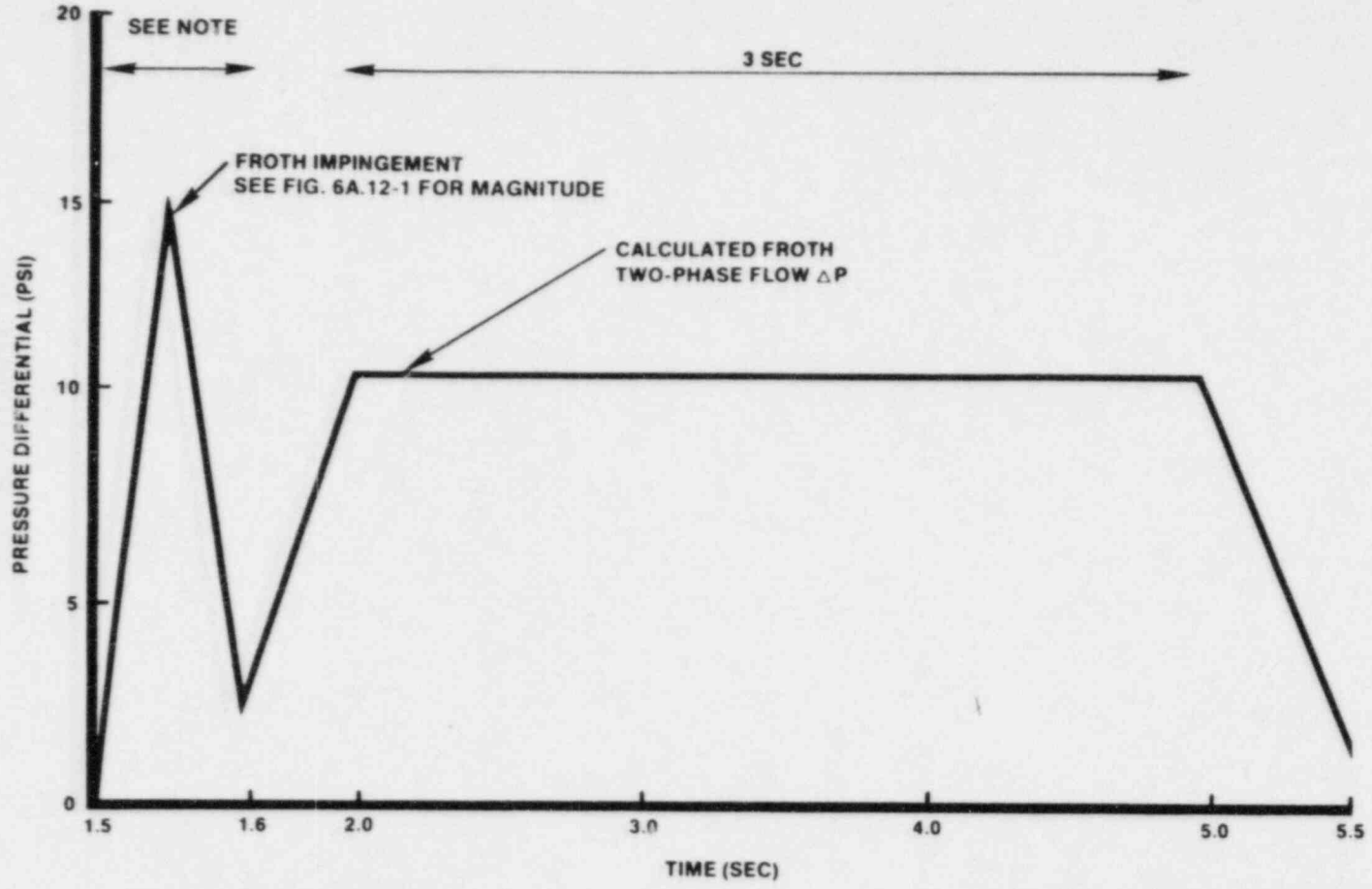

REF: GESSAR FIG. 3B-74

NOTE: DURATION CHOSEN TO GIVE THE MAXIMUM DYNAMIC LOAD FACTOR, BUT NOT LESS THAN 50 MSEC FOR EXPANSIVE STRUCTURES IMPACT

FIGURE 6A.11-1

LOADS ON HCU FLOOR
DUE TO POOL-SWELL FROTH IMPACT
AND TWO-PHASE FLOW

RIVER BEND STATION
FINAL SAFETY ANALYSIS REPORT

6A.12 LOADS ON STRUCTURES AT AND ABOVE THE HCU FLOOR ELEVATION

Structures at the HCU floor elevation experience "froth" pool swell which involves both impingement and drag type forces. GESSAR Fig. 3B-12 shows the loading sequences. Only structures in the line of sight of the pool experience froth pool swell loads. 15

The froth impingement load is applicable to structures between 19 ft above the initial pool surface and at and above the HCU floor. The forcing function is an isoceles triangle with a maximum amplitude shown on Fig. 6A.12-1. The pulse duration is chosen so as to give the maximum dynamic load factor for a triangular pulse. For elongated structures (i.e., pipes and beams) that span the entire pool, pulse durations less than 50 milliseconds need not be considered. Gratings are not subjected to these impingement loadings. 15

As discussed in Section 6A.6.1.6, following the initial froth impingement there is a period of froth flow through the annulus restriction at this elevation.

The froth flow pressure differential load (i.e., drag type force) specification of Fig. 6A.11-1 is based on an analysis of the transient pressure in the space between the pool surface and the HCU floor. The value of 11 psi is from the GESSAR analysis that assumes that the density of the flow through the annulus restriction is the homogenous mixture of the top 9 ft of the suppression pool water and the free air between the HCU floor and the pool (i.e., 18.8 lbm/cu ft). This is a conservative density assumption confirmed by the PSTF 1/3 scale tests which show an average density of approximately 10 lbm/cu ft. Representative tests of the expected Mark III froth conditions at the HCU floor are the 5-ft submergence tests of Series 5801, 5802, 5803, and 5804. GESSAR Reference 11 indicates the HCU floor pressure differential during these tests was in the 3 to 5 psi range (drag load on HCU floor). The River Bend Station analysis conducted with the LOCTVS analytical model predicts a froth flow pressure differential of 3.4 psi. 15 15 15

Structures above open areas at the HCU floor also experience loads. The impingement loads described above apply to an elevation 26 ft above the initial pool surface for flat structures and to 28.5 ft above for pipes.[1] The drag-type loads apply to structures up to 30 ft above the initial pool surface. The drag force can be reduced for structures more than 20 ft above the pool surface by multiplying by $(V/50)^2$, 15

[1] These impingement loads may be reduced by the ratio of grating open area to total area for structures above grated areas.

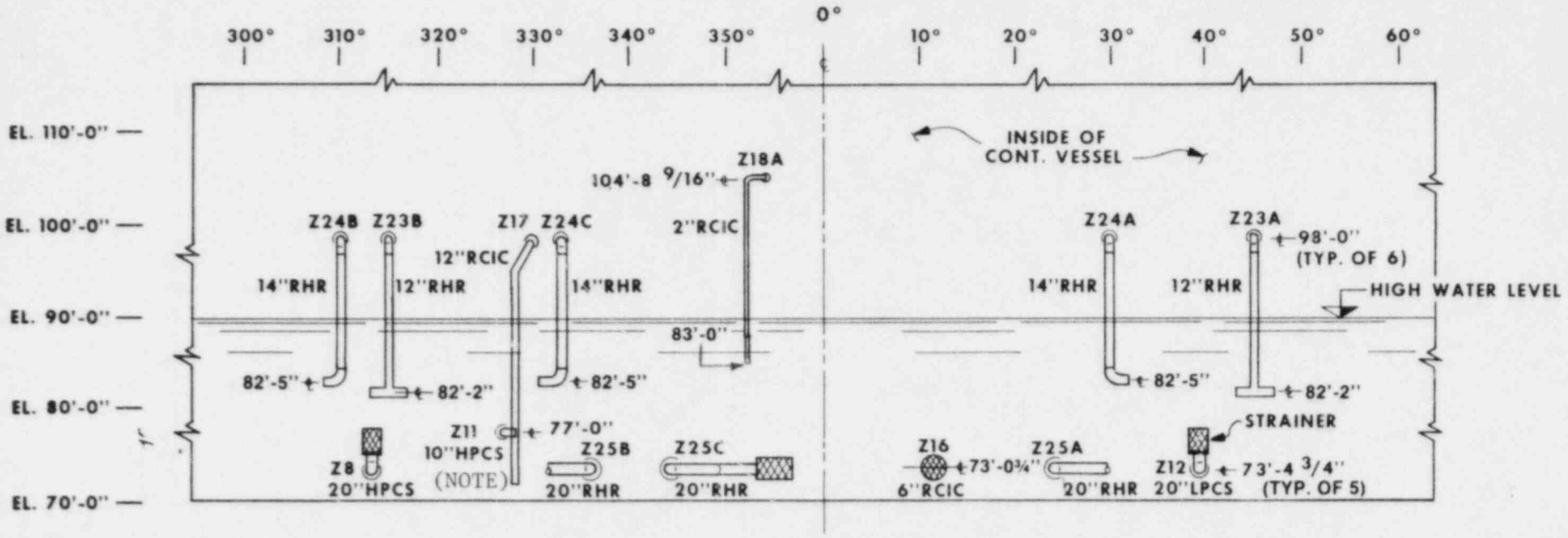

NOTE: See Figure 5.4-9a for details of sparger on this 12" RCIC line

FIGURE 6A.16-2

SUPPRESSION POOL PIPING
DEVELOPED ELEVATION

RIVER BEND STATION
FINAL SAFETY ANALYSIS REPORT

TABLE A.6A.5-1

QUENCHER BUBBLE PRESSURE
RIVER BEND STATION
~~90-90~~ 95-95% CONFIDENCE LEVEL)

Case Description	Design Value Bottom Maximum Pressure (psid) P(+)	P(-)	Ratio of P(-) and P(+)
Single valve subsequent actuation, at 120°F pool temperature	16.56	-7.41	0.45
Two adjacent valves first actuation, at 100°F pool temperature	9.66	-6.10	0.63
16 valves (all valve case) first actuation, at 100°F pool temperature	11.12	-6.09	0.55
7 ADS valves first actuation at 120°F pool temperature	9.72	-6.14	0.63

15

determining the attenuated bubble pressure at Point "A" for the multiple S/R valve cases.

For local peak containment pressure loading, there is significant reduction in pressure at certain locations when considering the time-sequenced phasing approach. The most limiting position on the containment is not affected (i.e., the local peak pressure is equal to the maximum bubble pressure - see Table A.6A.5-1). In addition, the 95-95 confidence level statistical analysis for the individual valve is conservatively applied to the multiple valve cases without consideration of the number of valves being actuated. In reality, the ~~90-90~~ confidence total load for the 16-valve case is much lower than that used in the local pool boundary load calculation. These two factors (i.e., time phasing and the multiple valve statistical consideration) have not been included in the development of the local pressure distributions on the containment wall, because they do not affect the limiting local pressure. However, these factors are important to the structural response and are employed in the building response evaluation. Attachment N describes the methodology used in developing structural responses for equipment evaluation.

15 | 95-95

15 |

$$Y = \sum_{\ell=1}^{M} \left[K_\ell \sum_{k=-N}^{N} \sum_{j=-N}^{N} \sum_{i=-N}^{N} \frac{(-1)^j \left(y - y_j^{(\ell)} \right)}{r^3_{ijk}} \right]$$

$$Z = \sum_{\ell=1}^{M} \left[K_\ell \sum_{k=-N}^{N} \sum_{j=-N}^{N} \sum_{i=-N}^{N} \frac{(-1)^j \left(z - z_k^{(\ell)} \right)}{r^3_{ijk}} \right] \quad \text{(L.6A-5)}$$

Where:

M = The number of sources in the pool (i.e., 43 air bubbles)

N = The total number of images considered for each source

K = Factor used for finite bubbles to satisfy the local pressure boundary condition at the real bubble surface (i.e., the pressure at the real bubble surface equals the independently calculated bubble pressure P_B).

The K factor is not a function of the structure location in the pool; it is a function of bubble radius and the bubble image function.

Insert

10. Number of Images

The results of a sensitivity study show that 7, 10, and 2 images in the vertical, radial, and circumferential directions, respectively, will provide adequate convergence. A typical arrangement of image sets in the vertical plane is shown on Fig. L.6A-5.

11. Direction of the Flow Field

The direction of the flow field at time t is determined by the unit vector $\vec{n}$ where:

Insert for page L.6A-7

The calculation of K is based on Reference 3, which is the same method as used in GESSAR (see GESSAR Reference 24). Calculated values of K as a function of time for RBS are shown in Table L.6A-1.

The standard drag force is calculated from

$$F_s(t) = C_D A_n \frac{\rho U_{\infty n}^2(t)}{2 g_c} \qquad \text{(L.6A-10)}$$

Where:

C_D = Drag coefficient for flow normal to the structure

A_n = Projected structure area normal to $U_{\infty n}(t)$

Add F_A and F_S at any time t to get the total load on the structure segment.

Insert →

The loads predicted by this procedure agree with the Mark III submerged structures test data (Reference 5). For additional conservatism, the final load is multiplied by a factor of 2 to cover the effects of a moving source.

The direction of total drag is normal to the submerged structures.

L.6A.2.4 Fallback Loads

There is no pressure increase on the suppression pool boundary during pool fallback (Section 6A.4.1.6). Structures within the containment suppression pool that are above the bottom vent elevation will experience drag loads as the water level subsides to its initial level. For design purposes, it is assumed that these structures will experience drag forces associated with water flowing at 35 ft/sec; this is the terminal velocity for a 20-ft freefall and is a conservative bounding number. Freefall height is limited by the HCU floor. The load computation procedure is the same as for calculating standard drag load in step 13 (Section L.6A.2.3) and will not be repeated here.

L.6A.2.5 LOCA Condensation Oscillations Loads

Steam condensation begins after the vent is cleared of water and the drywell air has been carried over into the wetwell. This condensation oscillation phase induces bulk water motion and therefore creates drag loads on structures submerged in the pool.

Insert for page L.6A-9

In accordance with NUREG-0978 acceptance criteria, non-cylindrical structures are modelled as circumscribed cylinders. To determine standard drag, Morrison's equation is used with a standard drag coefficient of not less than 1.2. If structures are found in the vicinity of each other, interference effects are evaluated and the drag coefficient increased accordingly.

The basis of the flow model for condensation oscillation load definition is derived from the work of Reference 4. The load calculation procedure is the same as for LOCA bubble loads given in Section L.6A.2.3 except for source strength and locations.

The condensation oscillation disturbances are modeled as phase point sources centered at the exit of each top vent. The source strength for calculating acceleration drag ($\dot{S}$) is determined from the Mark III $1/\sqrt{3}$ scale test data to be 188 ft^3/sec^2. The time history follows the wall pressure time history presented in Section 6A.4.1.5 which produces a frequency range of 2 to 3.5 Hz. The source strength for the velocity drag (S) is determined from the time integration of $\dot{S}$ time history. Since the sources are considered points, no adjustment for finite bubbles is required so the K factor of Equation L.6A-5 is set equal to 1.

L.6A.2.6 LOCA Chugging Loads

Chugging occurs after drywell air has been purged and the vent mass flux falls below a critical value. Chugging then induces acoustic pressure loads on structures submerged in the pool.

Insert →

The basis of the flow model for chugging load definition is derived from the work of Reference 4.

The loads on submerged structures due to chugging are calculated from the following procedure:

1. Locate the bubble center at 2.0 ft above the top vent centerline.

2. Determine location of structure (x, y, z) relative to bubble center (Fig. L.6A-6).

3. Calculate distance r from chugging center to a structure from

$$r = \sqrt{x^2 + y^2 + z^2}$$

4. Evaluate angle (θ) between structure axis and $\vec{r}$ from

$$\cos 0 = \cos \alpha_s \cos \alpha_b + \cos \beta_s \cos \beta_b + \cos \gamma_s \cos \gamma_b$$

Insert for page L.6A-10

In accordance with NUREG-0978 acceptance criteria (Appendix C, Section 2.0), circumscribed cylinders are used for non-cylindrical structures. In addition, standard drag is calculated and combined with the acceleration drag for all structures. The standard drag is calculated using Morrison's equation, with a drag coefficient of not less than 1.2. Structural interference effects are also evaluated when structures are found in the vicinity of each other. Table L.6A-2 provides the maximum velocity in the suppression pool. In accordance with Criteria 2.14.2 (2a) of the Mark I acceptance criteria, a standard drag coefficient of 3.6 is used for structures that do not satisfy the condition:

$$\frac{U_m T}{D} \leq 2.74$$

where: Um = maximum velocity
T = period of condensation oscillation
D = cylinder diameter

A 2-inch RCIC minimum flow line is the only structure which does not satisfy the exclusion condition. A standard drag coefficient of 3.6 is used in the submerged structure load evaluation for this line.

Table L.6A-1

K vs Time

Time (sec)	K
0.0	0.6887
0.05	0.5232
0.085	0.4440
0.090	0.4350
0.098	0.4222
0.102	0.4155
0.110	0.4026
0.115	0.3917
0.119	0.3905
0.152	0.3529
0.200	0.3147
0.230	0.2972
0.295	0.2697
0.340	0.2566
0.395	0.2447
0.429	0.2389
0.555	0.2239
0.600	0.2200
0.793	0.2065
0.911	0.1987
1.040	0.1908
1.091	0.1881

Table L.6A-2

Maximum Condensation Oscillation Velocities
in the Suppression Pool

Distance from Drywell Wall (ft)	Maximum Velocity, Um (ft/sec)	$D = \frac{U_m T}{2.74}$ (ft)
3.0	2.6	0.5
5.0	1.58	0.3
18.0	0.96	0.175

Period = 0.5 seconds
Frequency = 2 Hz